Cyclic Voltammetry of Palladium(II) Complexes with Tridentate Arsine Ligands. Separation of the Two Single-Electron Transfer Steps of the Pd(II) ↔ Pd(0) Interconversion Based on Thermodynamic and Kinetic Discrimination

Alison J. Downard,*,† Alan M. Bond,*,‡ Andrew J. Clayton,† Lyall R. Hanton,§ and David A. McMorran§

Department of Chemistry, University of Canterbury, Christchurch, New Zealand, Department of Chemistry, Monash University, Clayton, Victoria 3168, Australia, and Department of Chemistry, University of Otago, Dunedin, New Zealand

Received May 30, 1996[⊗]

A detailed electrochemical study of the reduction of the five-coordinate complexes $[Pd(mtas)_2]^{2+}$ and $[Pd(ptas)_2]^{2+}$ (mtas = bis(2-(dimethylarsino)phenyl)methylarsine; ptas = bis(2-(dimethylarsino)phenyl)phenylarsine) has been undertaken in acetonitrile and dichloromethane. When cyclic voltammetry is carried out in acetonitrile at room temperature using conventional scan rates, the main voltammetric feature is a single apparently quasireversible two-electron reduction step. A small peak due to reduction of the Pd(I) dimer $[Pd_2(L_3)_2]^{2+}$ (L_3 = mtas, ptas) formed in a follow-up reaction is also observed. At lower temperatures and faster scan rates, splitting of the two-electron reduction and associated oxidation peak occurs, enabling the thermodynamics and kinetics of the individual one-electron steps to be examined. The intermediate monomeric Pd(I) species are thermodynamically unstable with respect to disproportionation, but slow (relative to the experimental time scale) electrode kinetics for the Pd(I/0) couples and slow kinetics for the disproportionation reaction enable separation of the responses for the Pd(II/I) and Pd(I/0) couples. In dichloromethane, the Pd(I) complexes are thermodynamically stable over potential ranges of *ca.* 180 and 20 mV for $[Pd(ptas)_2]^+$ and $[Pd(mtas)_2]^+$, respectively. Examination of the electrochemical data allows rationalization of the trends in stabilities of the Pd(I) species.

Introduction

The redox chemistry of Pd is dominated by two-electron conversions between Pd(0), Pd(II), and Pd(IV) species.[1,2] Mononuclear Pd(I) complexes are rare because disproportionation to Pd(II) and Pd(0) is usually thermodynamically and kinetically favorable.[3,4] A recent study of the electrochemistry of five-coordinate nickel(II) triarsine complexes $[Ni(L_3)_2]^{2+}$ (L_3 = bis(2-(dimethylarsino)phenyl)methylarsine (mtas)[5] and bis-(2-(dimethylarsino)phenyl)phenylarsine (ptas)[6]) showed that all

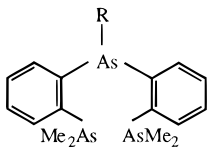

R = Me; mtas
= Ph; ptas

oxidation states from Ni(0) to Ni(IV) are thermodynamically and kinetically stable on the cyclic voltammetric time scale.[7] Importantly, the Ni(I) complexes are stable in acetonitrile over the unusually wide potential range of ca. 600 mV. Thus it was of interest to investigate whether the same coordination spheres would also stabilize the more unusual monomeric Pd(I) center.

Complexes $[Pd(mtas)_2]^{2+}$ and $[Pd(ptas)_2]^{2+}$ have recently been prepared and characterized.[5,8] X-ray structural analysis shows that $[Pd(mtas)_2](ClO_4)_2$ adopts a distorted square-pyramidal structure with a pendent terminal $-AsMe_2$ group, isomorphous with $[Ni(mtas)_2](ClO_4)_2$. Variable-temperature ^1H NMR studies indicate that both Pd(II) complexes are five-coordinate in solution and exchange processes occur between the pendent arsenic and some of the coordinated arsenic donors.[8]

This paper concerns the reductive electrochemistry of the complexes $[Pd(mtas)_2]^{2+}$ and $[Pd(ptas)_2]^{2+}$. Initial experiments revealed that unlike the Ni(II) complexes, the Pd(II) complexes exhibit only a single two-electron reduction step when cyclic voltammetry is carried out at room temperature in acetonitrile using conventional scan rates. However, for the Ni system the potential separation between the two reduction steps, $\Delta E_{1/2}$ ($=E_{1/2(II/I)} - E_{1/2(I/0)}$) was found to depend on the solvent, and the electrode kinetics of the Ni(I/0) couple appeared significantly slower than those of the Ni(II/I) couple.[7] Thus it was anticipated that correct choice of experimental conditions might lead to either thermodynamic or kinetic discrimination[9] of the two individual one-electron steps of the Pd(II) ↔ Pd(0) intercon-

† University of Canterbury.
‡ Monash University.
§ University of Otago.
⊗ Abstract published in *Advance ACS Abstracts,* November 1, 1996.

(1) Cotton, F. A.; Wilkinson, G. *Advanced Inorganic Chemistry: a Comprehensive Text,* 5th ed.; Wiley: New York, 1988; pp 917−937.
(2) Wilkinson, G., Gillard, R. D., McCleverty, J. A., Eds. *Comprehensive Coordination Chemistry*; Pergamon: London, 1987; Vol. 5.
(3) (a) Broadley, K.; Lane, G. A.; Connelly, N. G.; Geiger, W. E. *J. Am. Chem. Soc.* **1983**, *105*, 2486. (b) Lane, G. A.; Connelly, N. G.; Geiger, W. E. *J. Am. Chem. Soc.* **1987**, *109*, 402.
(4) Miedaner, A.; Haltiwanger, R. C.; Du Bois, D. L. *Inorg. Chem.* **1991**, *30*, 417.
(5) Cunninghame, R. G.; Nyholm, R. S.; Tobe, M. L. *J. Chem. Soc., Dalton Trans.* **1972**, 229.
(6) Fitzpatrick, M. G.; Hanton, L. R.; McMorran, D. A. *Inorg. Chem.* **1995**, *34*, 4821.
(7) (a) Downard, A. J.; Hanton, L. R.; Paul, R. L. *J. Chem. Soc., Chem. Commun.* **1992**, 235. (b) Downard, A. J.; Hanton, L. R.; McMorran, D. A.; Paul, R. L. *Inorg. Chem.* **1993**, *32*, 6028.
(8) McMorran, D. A. Ph.D. Thesis, University of Otago, Dunedin, New Zealand, 1995.
(9) For a thorough discussion of the concepts of thermodynamic and kinetic discrimination of the single-electron-transfer events of a two-electron-transfer reaction, see: Pierce, D. T.; Geiger, W. E. *J. Am. Chem. Soc.* **1992**, *114*, 6063.

S0020-1669(96)00642-8 CCC: $12.00

version, giving separate responses for the Pd(II/I) and Pd(I/0) couples. We describe here an electrochemical study of the Pd triarsine complexes that identifies conditions under which separate responses are observed for the two couples. Interestingly, depending on the experimental conditions, the basis of the discrimination is found to switch between thermodynamic and kinetic control. This enables factors important for the thermodynamic stabilization of monomeric Pd(I) complexes to be deduced. The study also provides another example of the manipulation of electrode kinetics to achieve separation of the single-electron transfer steps of an overall two-electron process when the intermediate oxidation state is thermodynamically unstable.[9]

Experimental Section

Syntheses. The ligands mtas[5] and ptas[6] and the complex $PdCl_2(MeCN)_2$[10] were prepared by published procedures.

$[Pd(mtas)_2](ClO_4)_2$. $PdCl_2(MeCN)_2$ (17 mg, 66 μmol) and excess $NaClO_4$ were stirred in acetone (10 mL) under N_2. Mtas (60 mg, 130 μmol) in acetone (10 mL) was added and the solution stirred for 20 min. During this time a deep red color developed and some white solid precipitated. The solid was removed by filtration, the solution pumped to dryness, and the residue taken up in 1:1 acetone/butanol. Slow evaporation gave $[Pd(mtas)_2](ClO_4)_2$ as red crystals. Yield: 61 mg (77%). ***Caution!*** Perchlorate salts may explode without warning. No explosions were experienced during this study. Anal. Calcd for $C_{34}H_{46}As_6PdCl_2O_8$: C, 33.76; H, 3.83. Found: C, 33.81; H, 3.80. ^{1}H NMR (CD_2Cl_2, δ, ppm), 298 K: 1.34 (s, 12H), 1.53 (s, 12H), 1.9 (s, 6H), 7.65−7.85 (m, 16H).^{13}C{^{1}H} NMR (DMF-d_7, δ, ppm), 298 K: 12.11, 13.9 (br), 20.0 (vbr), 130.5 (br), 131.6 (br), 132.0 (br), 132.9 (br), 139.0 (br), 140.8 (vbr).

$[Pd(ptas)_2](PF_6)_2$. The synthesis was similar to that described above, using excess NH_4PF_6 in place of $NaClO_4$ and extending the reaction time to 1 h. Crystallization from 1:1 acetone/butanol gave bright red crystals of $[Pd(ptas)_2](PF_6)_2$. Yield: 67%. Anal. Calcd for $C_{44}H_{50}As_6PdCl_2F_{12}$: C, 32.15; H, 3.55. Found: C, 31.58; H, 3.55. ^{1}H NMR (DMF-d_7, δ, ppm), 298 K: 1.7 (s, vbr, 24H), 7.3−8.3 (m, br, 26H).^{13}C{^{1}H} NMR (DMF-d_7, δ, ppm), 298 K: 15.9 (br), 132.44, 133.74, 133.84, 134.53, 134.76, 134.97, 135.50, 139.45, 143.9 (br).

Solvents and Electrolytes. Solvents used for electrochemistry were of analytical reagent grade and were dried immediately prior to use either by passing through a column of activated alumina or by distillation from P_2O_5 as described previously.[7b] Tetrabutylammonium hexafluorophosphate (Bu_4NPF_6) was prepared by following a literature procedure[11] and was oven-dried at 100 °C.

Electrochemical Instrumentation and Methods. Cyclic voltammetric measurements were made using either a Cypress Systems Model CS-1090 computer-controlled electroanalytical system, a BAS 100 electrochemical analyzer or a PAR Model 174A polarographic analyzer coupled to a PAR Model 175 universal programmer and a Graphtec WX 1200 recorder. Working electrodes were glassy carbon (GC) or Pt disks (area = 7.0 and 0.8 mm^2, respectively) and GC fiber or Pt disk microelectrodes (11 and 25 μm diameter, respectively). The auxiliary electrode was a Pt wire and a Ag/Ag^+ (0.01 M in CH_3CN−0.1 M Bu_4NPF_6) reference electrode was used. Potentials are reported *vs* ferrocenium/ferrocene (Fc^+/Fc) after referencing to *in situ* ferrocene. All solutions were degassed with nitrogen prior to measurement. For experiments performed at subambient temperatures, dry ice/acetone and dry ice/acetonitrile slush baths were employed giving temperatures of −70 and −40 °C, respectively.

Controlled-potential electrolysis was performed using a PAR Model 273 potentiostat/galvanostat and a three-compartment cell. The Pt mesh working and auxiliary electrodes were separated by a porosity 5 glass frit and the working and reference electrodes (described above) were separated by a Vycor frit. A 5 mL aliquot of 0.5 mM $[Pd(mtas)_2]^{2+}$ in acetonitrile−0.1 M Bu_4NPF_6 was electrolyzed at an applied potential of −1.4 V *vs* Fc^+/Fc. A nitrogen atmosphere was maintained in the cell, the solution was stirred and light was excluded throughout the electrolysis. Progress of the electrolysis was monitored by steady-state voltammetry at a GC fiber microelectrode. After 90% consumption of starting material, the light green solution was rotary evaporated to dryness, the resulting solid carefully redissolved in ethyl acetate, and the green solution separated from the less soluble supporting electrolyte. After the solvent was removed, this procedure was repeated three times.

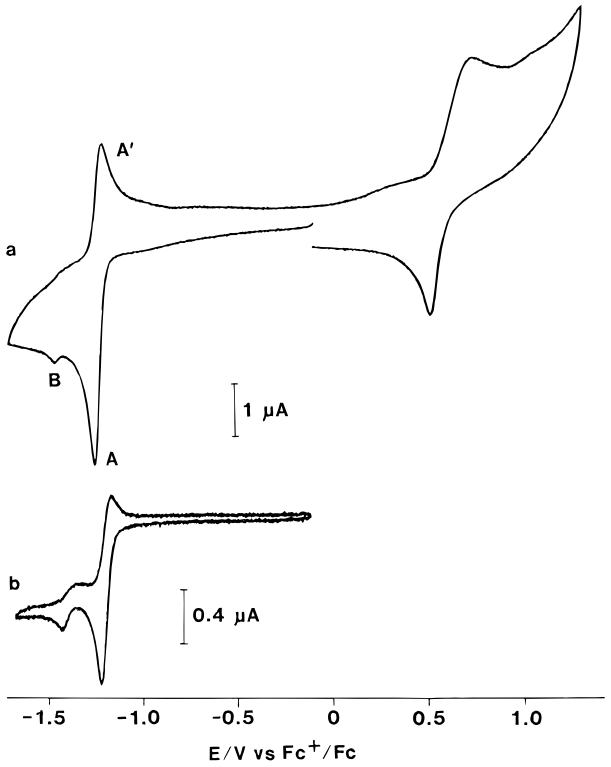

Figure 1. Cyclic voltammograms recorded in acetonitrile−0.1 M Bu_4NPF_6 (T = 22 °C) of 0.63 mM $[Pd(mtas)_2]^{2+}$ at a GC electrode and scan rates of (a) 0.1 and (b) 0.01 V s^{-1}.

Electrospray Mass Spectrometric Analysis of the Electrolysis Product. Electrospray mass spectra were collected in the positive ion mode using a VG Bio-Q triple quadrupole mass spectrometer and a 2-propanol/water (50:50) mobile phase. The sample was dissolved in dichloromethane (*ca.* 0.1 mM) and injected into the spectrometer via a Rheodyne injection valve (sample loop 10 μL). The voltage at the first skimmer electrode (B1) was 50 V.

Results and Discussion

Cyclic Voltammetry at 22 °C and Scan Rates ≤1 V s^{-1} in Acetonitrile−Bu_4NPF_6. Initial investigations of the electrochemistry of $[Pd(mtas)_2]^{2+}$ and $[Pd(ptas)_2]^{2+}$ were undertaken in acetonitrile−0.1 M Bu_4NPF_6 at scan rates between 0.01 and 1 V s^{-1}. The responses of the complexes were qualitatively similar; Figure 1a shows the cyclic voltammogram recorded at a glassy carbon (GC) electrode for 0.63 mM $[Pd(mtas)_2]^{2+}$ at v = 0.1 V s^{-1}. The main features of the voltammogram are a two-electron oxidation step at positive potentials and a two-electron reduction step (labeled A/A′) at negative potentials, followed by a small reduction peak (B) at even more negative potentials. Assignment of the number of electrons is based on comparison of the cyclic voltammetric peak currents with those of analogous Ni complexes which undergo single electron transfers.[7] Coulometry could not be used to confirm the assignment due to the follow-up reactions described below. Thus

(10) Heck, R. F. *Palladium Reagents in Organic Synthesis;* Academic Press: London, 1985.
(11) Kissinger, P. T., Heineman, W. R., Eds. *Laboratory Techniques in Electroanalytical Chemistry*; Marcel Dekker: New York, 1984; p 378.

the oxidation process is assumed to lead to the formation of a Pd(IV) complex with an accompanying increase in coordination number from 5 to 6. Pseudooctahedral coordination may be achieved via coordination of either the pendent $-AsMe_2$ group or MeCN. The details of the oxidation processes were not examined further.

The two-electron reduction process can reasonably be assigned to the formation of a Pd(0) center with coordination number between 2 and 4 (or to an equilibrium mixture of several Pd(0) species).[1,2] There are many examples of stable Pd(0) complexes; particularly relevant is $[Pd(diars)_2]^0$ (diars = 1,2-bis(dimethylarsino)benzene), which is sufficiently stable to be isolated as the solid.[12] The dominant features of the cyclic voltammograms of both complexes are therefore described by eq 1, where CN = coordination number; L_3 = ptas, mtas; n =

$$\underset{CN = 2-4}{[Pd(L_3)_{2-n}]^0} \overset{\text{peak A}\ 2e^-}{\underset{\text{peak A}'}{\rightleftharpoons}} \underset{CN = 5}{[Pd(L_3)_2]^{2+}} \overset{-2e^-}{\rightleftharpoons} \underset{CN = 5, 6}{[Pd(L_3)_2]^{4+}} \quad (1)$$

0 or 1 and peaks A and A′ are as indicated in Figure 1a.

For both Pd(II/0) couples, the potential separation between the peaks (ΔE_p) is greater than expected for a reversible two-electron step (28.5 mV at 25 °C),[13] suggesting the involvement of closely-spaced stepwise electron transfers, slow electrode kinetics, and/or coupled homogeneous reactions.[14] Despite careful attempts to reproduce experimental conditions and electrode surface cleanliness, large variations in ΔE_p values (indicating large variations in apparent electron transfer rates) were observed during the study, but most often, the apparent kinetics of the electrode processes were faster at GC than Pt. This observation is discussed in more detail below.

The origin of the small cathodic peak, B, which follows the main reduction process was examined by varying the cyclic voltammetric scan rate and the concentration of the complex. Figure 1b shows a cyclic voltammogram recorded at GC of 0.63 mM $[Pd(mtas)_2]^{2+}$ at $\upsilon = 0.01$ V s^{-1}. The increase in the size of peak B relative to A as the scan rate decreases is consistent with the slow formation of a reducible species arising from the major reduction product. At constant scan rate the amount of product formed was not dependent on the concentration of the complex over the range 0.25−2.5 mM indicating that the rate-determining step for product formation is first order and not higher order. The nature of the product and its mechanism of formation are described in the next section.

Controlled-Potential Bulk Electrolysis of $[Pd(mtas)_2]^{2+}$ and Electrospray Mass Spectrometric Identification of the Reduction Product. Controlled-potential bulk electrolysis of 5 mL of 0.5 mM $[Pd(mtas)_2]^{2+}$ in acetonitrile−0.1 M Bu_4NPF_6 was undertaken at 22 °C using a Pt-mesh working electrode at an applied potential of −1.4 V *vs* Fc^+/Fc. Light was excluded from the cell, and progress of the electrolysis was monitored by steady-state voltammetry at a GC fiber microdisk electrode. (In addition to indicating the extent of reaction, steady-state voltammetry shows the oxidation state of electrolysis products, information not easily obtained from cyclic voltammetry.) After consumption of charge corresponding to 2.3 faradays mol^{-1}, the yellow solution had become light green and the electrolysis current was very small. Steady-state voltammetry (not shown, see Supporting Information) revealed that approximately 10% of the starting complex remained and the solution now contained an electroactive species with $E_{1/2} \simeq -1.45$ V (i.e. corresponding to the second reduction peak (B) in the cyclic voltammograms). The steady-state plateau current for reduction of this species is approximately half that due to the two electron reduction of $[Pd(mtas)_2]^{2+}$ in the starting solution. This suggests that the product is formed almost quantitatively and undergoes a further one-electron reduction per Pd center. After electrolysis, large ill-defined oxidation waves are seen positive of 0.5 V; these are attributed to irreversible oxidation of the free ligand (E_p^a = 0.83 and 1.20 V *vs* SCE at $\upsilon = 0.1$ V s^{-1}).[7]

Solvent was removed from the light green solution and the residue extracted with ethylacetate to remove the electrolyte. After being dissolved in dichloromethane, the residue was examined by electrospray mass spectrometry in the positive ion mode, giving a major peak at $m/z = 559$ and a small peak at $m/z = 1262$. Comparisons with the expected isotope patterns[15] enabled these major peaks to be assigned to the Pd(I) dimer $[Pd_2(mtas)_2]^{2+}$ and its PF_6^- adduct $[Pd_2(mtas)_2PF_6]^+$, respectively.

Close to quantitative formation of the Pd(I) dimer thus occurs on the bulk electrolysis time scale while the amount detected during cyclic voltammetric measurements depends on the scan rate. The dimer can be reduced in an irreversible two-electron step (i.e. one-electron per Pd center), analogous to the electrochemical behavior observed for the Pd(I)−triphosphine dimer $[Pd(etp)]_2(BF_4)_2$ (etp = bis[(diphenylphosphino)ethyl]phenylphosphine).[16] Formation of the triarsine dimer presumably occurs via comproportionation of a Pd(0) species with the Pd(II) starting complex. Athough the mechanistic details are not known, the overall reaction can be represented by eq 2. The

$$2[Pd(mtas)_2]^{2+} + 2e^- \rightarrow [Pd_2(mtas)_2]^{2+} + 2mtas \quad (2)$$

theoretical charge required for reaction 2 is 1 faraday mol^{-1}, considerably less than the 2.3 faradays mol^{-1} consumed in the bulk electrolysis. Reaction of a Pd(0) complex with adventitious O_2 or other components of the solution may account for this.

Molecular modeling was employed to investigate possible structures for the dimer. Two structures were examined: a dimer in which each triarsine ligand bridges the two metal centers and also chelates and a dimer containing only chelating ligands. Energy-minimization using the molecular modeling program CAChe[17] (based on an MM2 force-field) determined that both isomers lie at low energy, with the bridged dimer lower. This structure is analogous to that determined for $[Pd(etp)]_2(BF_4)_2$[16] which also contains a tridentate ligand. However, it is clear from literature reports[18] that the factors which determine the structures of Pd(I) dimers are subtle, and hence either structural type might be anticipated.

Cyclic Voltammetry in Acetonitrile−Bu_4NPF_6 at T < 22 °C and Scan Rates >1 V s^{-1} and in Dichloromethane−Bu_4NPF_6. The overall two-electron reduction of the Pd complexes is expected to take place in discrete one-electron steps. As noted in the Introduction, observation of separate responses for the individual single electron transfers might be

(12) Chatt, J.; Hart, F. A.; Watson, H. R. *J. Chem. Soc.* **1962**, 2537.
(13) Bard, A. J.; Faulkner, L. R. *Electrochemical Methods*; Wiley: New York, 1980; p 229.
(14) Reference 13, pp 232−235.
(15) Arnold, L. J. Isotope computer program for the Macintosh. University of Waikato, 1994.
(16) Du Bois, D. L.; Miedaner, A.; Haltiwanger, R. C. *J. Am. Chem. Soc.*, **1991**, *113*, 8753.
(17) CAChe Scientific, Inc., PO Box 4003, Beaverton, OR.
(18) See, for example, refs 4 and 16 and also: (a) Tanase, T.; Kawahara, K.; Ukaji, H.; Kobayashi, K.; Yamazaki, H.; Yamamoto, Y. *Inorg. Chem.* **1993**, *32*, 3682. (b) Kullberg, M. L.; Lemke, F. R.; Powell, D. R.; Kubiak, C. P. *Inorg. Chem.* **1985**, *24* 3589. (c) Holloway, R. G.; Penfold, B. R.; Colton, R.; McCormick, M. J. *J. Chem. Soc., Chem. Commun.* **1976**, 485.

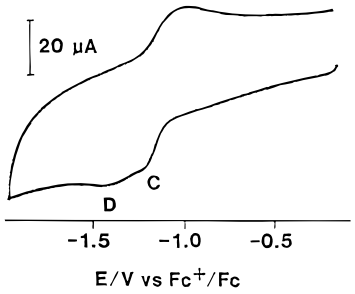

Figure 2. Cyclic voltammogram recorded in acetonitrile−0.1 M Bu_4NPF_6 ($T = 22$ °C) of 0.43 mM $[Pd(ptas)_2]^{2+}$ at a GC electrode and $v = 50$ V s^{-1}.

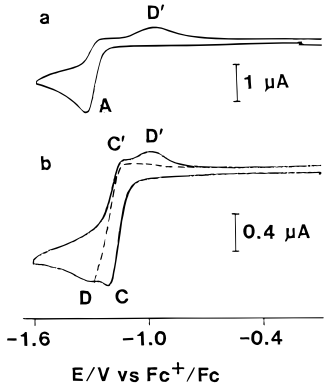

Figure 3. Cyclic voltammograms recorded in acetonitrile−0.1 M Bu_4NPF_6 ($T = -40$ °C) using a Pt electrode of (a) 0.5 mM $[Pd(mtas)_2]^{2+}$ ($v = 0.1$ V s^{-1}) and (b) 0.5 mM $[Pd(ptas)_2]^{2+}$ ($v = 0.05$ V s^{-1}).

achieved via manipulation of the thermodynamics or electrode kinetics of one or both steps by correct choice of the experimental conditions. Hence reduction of the Pd(II) complexes was examined in acetonitrile−0.1 M Bu_4NPF_6 at scan rates up to 50 V s^{-1} and temperatures down to −40 °C and in dichloromethane−0.1 M Bu_4NPF_6 at temperatures between 22 and −70 °C. For $[Pd(mtas)_2]^{2+}$ in acetonitrile solution, increasing the scan rate leads to the disappearance of the peak for the reduction of $[Pd_2(mtas)_2]^{2+}$ and to broadening of the return oxidation peak. In contrast, two closely spaced peaks (C and D, Figure 2) are easily discerned for the overall two-electron reduction of $[Pd(ptas)_2]^{2+}$. As the temperature is lowered, voltammograms recorded at $v = 0.1$ V s^{-1} in an acetonitrile solution of $[Pd(mtas)_2]^{2+}$ exhibit broadening of peak A while the associated oxidation peak shifts progressively to more positive potentials. The limiting behavior at −40 °C is shown in Figure 3a. For $[Pd(ptas)_2]^{2+}$ (Figure 3b), two closely-spaced peaks are observed for both the reduction (peaks C and D) and coupled oxidation process (peaks C′ and D′). When the scan is reversed after peak C only peak C′ is seen on the return scan.

Using dichloromethane as the solvent and 0.1 M Bu_4NPF_6 as electrolyte, the reduction of $[Pd(mtas)_2]^{2+}$ shows a distorted peak shape even at the slowest scan rate (0.02 V s^{-1}) and at $v = 0.1$ V s^{-1} (Figure 4a) there is clear evidence of two merged reduction peaks, C and D. Peak B is due to reduction of the dimer $[Pd_2(mtas)_2]^{2+}$. As the scan rate becomes faster, increasing distortion then splitting of the coupled oxidation process is observed; Figure 4b shows the response at $v = 5$ V s^{-1}. Scan reversal after the first reduction peak (C) gives an associated oxidation peak at C′.

Cyclic voltammograms of $[Pd(ptas)_2]^{2+}$ at slow scan rates in dichloromethane−0.1 M Bu_4NPF_6 show three reduction steps (peaks B, C, and D, Figure 5a). The clear separation of peak C enables measurement of its current and assignment to a one-electron process. Peak B is due to reduction of $[Pd_2(ptas)_2]^{2+}$;

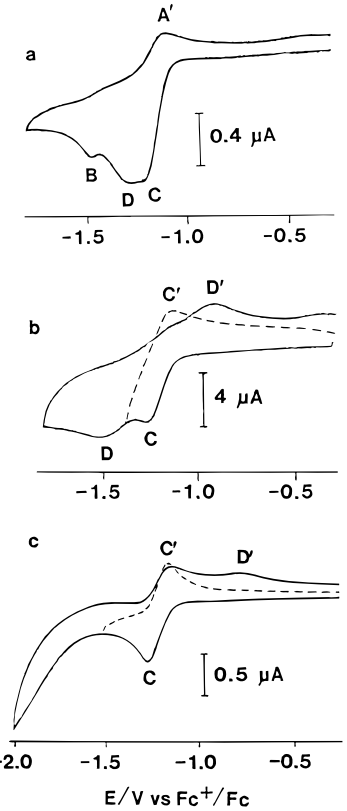

Figure 4. Cyclic voltammograms of 0.5 mM $[Pd(mtas)_2]^{2+}$ recorded in dichloromethane−0.1 M Bu_4NPF_6 using a Pt electrode and scan rates of (a) 0.1 V s^{-1} ($T = 22$ °C), (b) 5 V s^{-1} ($T = 22$ °C), and (c) 0.1 V s^{-1} ($T = -70$ °C).

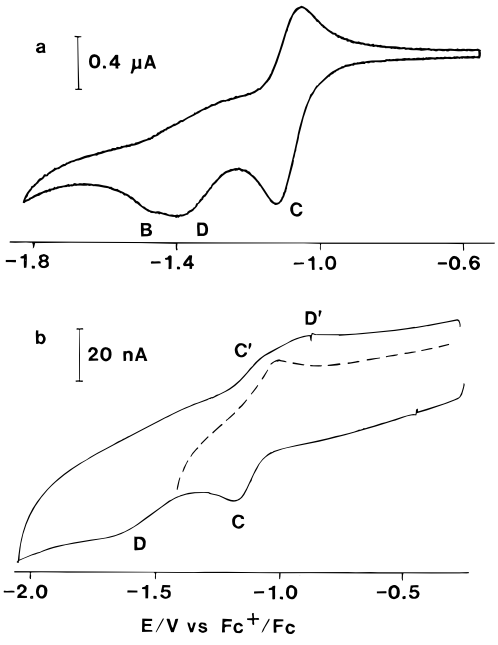

Figure 5. Cyclic voltammograms of 0.5 mM $[Pd(ptas)_2]^{2+}$ recorded in dichloromethane−0.1 M Bu_4NPF_6 ($T = 22$ °C) at scan rates of (a) 0.05 V s^{-1} (Pt electrode) and (b) 50 V s^{-1} (Pt microelectrode).

consistent with this interpretation, the peak becomes relatively smaller as the scan rate increases. At $v = 50$ V s^{-1} the oxidation process on the reverse scan is also seen as two closely spaced peaks (Figure 5b). Scan reversal after the first reduction peak results in a uncomplicated C/C′ couple.

As the solution temperature is lowered, analogous behavior is exhibited by both complexes. The second reduction peak (D) moves progessively to more negative potentials and the

associated oxidation peak (D′) more positive. Figure 4c shows a voltammogram for $[Pd(mtas)_2]^{2+}$ recorded at −70 °C. At this temperature, the second reduction process has merged with the solvent background but scans into this region give rise to oxidation peak D′, indicating that further reduction of the complex occurs simultaneously with reduction of the solvent. When the scan is reversed before the negative solvent limit, an unperturbed single-electron redox couple is observed (C/C′).

In summary, as the experimental conditions are varied, the response for both complexes ranges from a single apparently quasireversible two-electron reduction/oxidation couple (peaks A/A′) to two clearly separated redox couples (peaks C/C′ and D/D′). Couple C/C′ is a chemically reversible one-electron process with relatively fast kinetics while couple D/D′ appears to have significantly slower kinetics. When the experimental time scale is sufficiently long, an additional peak (B) due to reduction of the dimer $[Pd_2(L_3)_2]^{2+}$ is evident.

Assignment of Couples C/C′ and D/D′. Interpretation of the electrochemical behavior is complicated by the overall two-electron nature of the reductive redox chemistry and the expected coupled structural change(s) from five-coordinate Pd(II) to two-, three-, or four-coordinate Pd(0). This allows the possibility that separate responses may arise from species of different oxidation states and from isomers of the same oxidation state. Comparisons with the electrochemical behavior of $[Ni(mtas)_2]^{2+}$ and $[Ni(ptas)_2]^{2+}$ suggest that only the former possibility is realized for the Pd complexes.[7] Two well-separated ($\Delta E_{1/2} \approx 800$ mV in dichloromethane and 600 mV in acetonitrile) chemically reversible one-electron reductions were observed for the Ni complexes over a range of scan rates and temperatures. The two processes were assigned to Ni(II/I) (kinetically fast) and Ni(I/0) (kinetically slow) couples. No additional features due to the participation of isomers with different coordination spheres were detected under any conditions, and thus the Ni(I/0) reduction was described as a one-step reaction[7,19,20] with a change in coordination number from 5 to 4 occurring in concert with the electron-transfer step. Unfortunately, theoretical differences between this case of simultaneous electron transfer and structural change and a square scheme with fast chemical reactions before and after electron transfer are often undetectable.[21] Our consideration of processes as one- or two-step reactions is therefore based on convenience rather than direct evidence.

Under conditions where two reduction couples are observed, the response of the Pd complexes clearly parallels that of the Ni complexes and hence is most reasonably described by eqs 3 and 4 where n = 0 or 1.

$$\text{peaks C/C}': \quad \underset{\text{CN}=5}{[Pd(L_3)_2]^{2+}} + e^- \rightleftharpoons \underset{\text{CN}=5}{[Pd(L_3)_2]^{+}} \qquad E_{1/2(II/I)} \tag{3}$$

$$\text{peaks D/D}': \quad \underset{\text{CN}=5}{[Pd(L_3)_2]^{+}} + e^- \rightleftharpoons \underset{\text{CN}<5}{[Pd(L_3)_{2-n}]^{0}} + n(L_3) \qquad E_{1/2(I/0)} \tag{4}$$

It should be noted that the larger ΔE_p values for the Pd(I/0) couples in comparison to the Pd(II/I) couples are not *necessarily* indicative of structural change accompanying the second rather than the first electron-transfer step. There are firmly established examples where reversible electrochemistry is not coupled to structural integrity and conversely where slow electron transfer appears not to arise from accompanying structural change.[4,7,19] The former situation has been treated theoretically, and the dangers of equating fast electrode kinetics with lack of structural change have been clearly illustrated.[21] However, considering the chemistry of the systems, it is reasonable to assume that the Pd(I) (and Ni(I)) complexes are five coordinate and a decrease in coordination number is coupled to the M(I/0) (M = Pd, Ni) redox reaction. Further, it is emphasised that the generally large ΔE_p values obtained for the Pd(I/0) couples are equated with low *apparent* rates of electron transfer at the electrode. The *actual* rate of the electron transfer step may be fast (with respect to the experimental time scale) with the coupled structural rearrangement rate-controlling.[21]

Thermodynamics of the Two One-Electron Steps. Thermodynamic details of the electron transfer steps can be deduced by examination of the voltammograms obtained over a range of experimental conditions. Electrochemical data are presented in Table 1. The reproducibility of ΔE_p values was poor and those reported are "typical" for conditions under which the associated $E_{1/2}$ values were obtained. Unfortunately the irreproducibility of response prevents meaningful digital simulation[22] of the experimental data and thereby determination of $E^{\circ\prime}$ for each redox reaction. Hence only $E_{1/2}$ values derived from averaging cyclic voltammetric reduction and oxidation peak potentials are accessible. Although $E_{1/2}$ need not necessarily be equated with $E^{\circ\prime}$ for the processes being considered, it is probably reasonable to assume that trends in $E_{1/2}$ values have thermodynamic significance.

Consideration of the voltammograms shown in Figure 3 suggests that in acetonitrile, $\Delta E_{1/2}$ ($E_{1/2(II/I)} - E_{1/2(I/0)}$) is negative for both complexes. This negative value of $\Delta E_{1/2}$ indicates that $[Pd(L_3)_2]^+$ is thermodynamically unstable, while a positive value would imply the species is stable with respect to disproportionation. $E_{1/2(II/I)}$ is significantly more negative than $E_{1/2(I/0)}$ for $[Pd(mtas)_2]^{2+}$ whereas for the ptas complex the difference in potentials is small. Thus peak A in Figure 3a corresponds to a two-electron reduction of $[Pd(mtas)_2]^{2+}$ which is the consequence of the thermodynamic instability of the intermediate one electron product, both to further reduction at the electrode and to disproportionation in solution (eq 5). On the

$$2[Pd(L_3)_2]^+ \rightarrow [Pd(L_3)_2]^{2+} + [Pd(L_3)_{2-n}]^0 + nL_3 \tag{5}$$

reverse scan, peak D′ arises from oxidation of $[Pd(mtas)_{2-n}]^0$ to $[Pd(mtas)_2]^+$ which is then further oxidized to $[Pd(mtas)_2]^{2+}$ at that potential. The $E_{1/2}$ value for the $[Pd(mtas)_2]^{+/0}$ couple cannot be established because the reduction component is not observable under the experimental conditions; however, it must be ≥ -1.15 V (the midway potential between peaks A and D′). For $[Pd(ptas)_2]^{2+}$ on the other hand, the scan in Figure 3b shows features arising from all four electron transfers. The midpoint between peaks D and D′ gives an approximate $E_{1/2(I/0)}$ and this is close to, but slightly positive of, $E_{1/2(II/I)}$. Peak C appears to be enhanced at the expense of D, consistent with disproportionation of the singly reduced complex.

Scans recorded in dichloromethane (Figures 4 and 5) show that in this electrolyte $\Delta E_{1/2}$ is positive for both complexes, i.e. $E_{1/2(I/0)}$ is more negative than $E_{1/2(II/I)}$. The difference in potentials is very small for $[Pd(mtas)_2]^{2+}$ and significantly larger for $[Pd(ptas)_2]^{2+}$. For both complexes the more negative potental for the second reduction step and the slower kinetics

(19) Geiger, W. E. In *Progress in Inorganic Chemistry*; Lippard, S. J., Ed.; John Wiley and Sons: New York, 1985; Vol. 33, p 275.
(20) Evans, D. H.; O'Connell, K. M. In *Electroanalytical Chemistry*; Bard, A. J., Ed.; Marcel Dekker: New York, 1986; Vol. 14, pp 113−207.
(21) (a) Bond, A. M.; Oldham, K. B. *J. Phys. Chem.* **1983**, *87*, 2492. (b) Bond, A. M.; Oldham, K. B. *J. Phys. Chem.* **1985**, *89*, 3739.
(22) Feldberg, S. W. In *Electroanalytical Chemistry. A Series of Advances*; Bard, A. J., Ed.; Marcel Dekker: New York, 1969; Vol. 3, pp 199−296.

Table 1. Cyclic Voltammetric Data Obtained at Pt Electrodes[a]

complex	solvent (0.1 M Bu_4NPF_6)	$E_{1/2}$/V[b] Pd(II/0)	$E_{1/2}$/V[b] Pd(II/I)	$E_{1/2}$/V[b] Pd(I/0)	E_p/V[c] $[Pd_2(L_3)_2]^{2+}$
$[Pd(mtas)_2]^{2+}$	CH_3CN	−1.21 (85)[c]	∼ −1.3 (∼80)[d]	≥ −1.1 (≤340)[d]	−1.46[c]
$[Pd(ptas)_2]^{2+}$	CH_3CN	−1.10 (72)[e]	−1.14 (60)[f]	−1.1 (300)[f]	−1.37[e]
$[Pd(mtas)_2]^{2+}$	CH_2Cl_2		−1.22 (160)[g]	−1.24 (580)[g]	−1.48[h]
$[Pd(ptas)_2]^{2+}$	CH_2Cl_2		−1.09 (70)[h]	−1.27 (840)[j]	−1.47[h]

[a] [complex] = 0.5 mM and T = 22 °C unless indicated otherwise. [b] $E_{1/2} = (E_p^a - E_p^c)/2$; V vs Fc^+/Fc; values in parentheses indicate ΔE_p values in mV, obtained under the conditions indicated. [c] [complex] = 0.63 mM; ν = 0.1 V s^{-1}. [d] ν = 0.1 V s^{-1}; T = −40°C. [e] [complex] = 0.43 mM; ν = 0.05 V s^{-1}. [f] ν = 0.05 V s^{-1}; T = −40°C. [g] ν = 5 V s^{-1}. [h] ν = 0.1 V s^{-1}. [j] ν = 50 V s^{-1}.

for this process result in the splitting of the reduction process into two peaks at all scan rates and temperatures examined. The peak potential for the oxidation of $[Pd(L_3)_{2-n}]^0$ is very close to that for oxidation of $[Pd(L_3)_2]^+$ for both complexes at slow scan rates at room temperature (Figures 4a and 5a), and hence the oxidation peak is observed at the same potential when the scan is reversed before or after reduction of $[Pd(ptas)_2]^+$ (Figure 4a). At faster scan rates (Figures 4b and 5b), the oxidation peak for the kinetically slow Pd(I/0) couple (peak D′) moves positive of that for the Pd(II/I) couple (peak C′). Oxidation of $[Pd(L_3)_{2-n}]^0$ to $[Pd(L_3)_2]^{2+}$ occurs at D′ because the intermediate one-electron product is thermodynamically unstable at that potential. For the ptas complex, comproportionation (eq 6) is thermodynamically favorable and leads to a small peak (C′) for oxidation of $[Pd(ptas)_2]^+$ when the forward scan extends past the second reduction step.

$$[Pd(L_3)_2]^{2+} + [Pd(L_3)_{2-n}]^0 + nL_3 \rightarrow 2[Pd(L_3)_2]^+ \quad (6)$$

Thus to summarize the thermodynamic properties of the systems, in acetonitrile, disproportionation of the Pd(I) complexes is thermodynamically favorable. Separation of the two single-electron steps of the $[Pd(ptas)_2]^{2+} \leftrightarrow [Pd(ptas)_{2-n}]^0$ conversion is based on the slow electrode kinetics of the Pd(I/0) couple; i.e., discrimination is due to kinetic factors. In dichloromethane the Pd(I) complexes are stable with respect to disproportionation. $[Pd(ptas)_2]^+$ has a stability range of *ca.* 180 mV enabling separate responses to be observed for the Pd(II/I) and Pd(I/0) couples. Only *ca.* 20 mV separates the two electron-transfer steps for $[Pd(mtas)_2]^{2+}$, and for this complex, manipulation of electrode kinetics is also required to see all features of the redox chemistry.

Examination of the data in Table 1 reveals two trends in $E_{1/2}$ values that deserve further comment. First, as noted above, for both complexes $\Delta E_{1/2}$ is negative in acetonitrile and positive in dichloromethane. The origin of these orderings is assumed to lie in the relative importance of solvent stabilization for complexes of different charges. Thus it is assumed that the stabilities of the Pd(I) and Pd(0) complexes are largely unaffected by solvent polarity whereas the divalent complexes will be relatively destabilized in the lower polarity solvent (dichloromethane) and hence reduced at more positive potentials. Consistent with this explanation, a smaller value for $\Delta E_{1/2}$ in acetonitrile than in dichloromethane was also observed for the analogous Ni complexes.[7]

Second, comparing the potentials for each complex in both solvents, $\Delta E_{1/2}$ is larger for $[Pd(ptas)_2]^{2+}$ than for $[Pd(mtas)_2]^{2+}$; i.e., it has a larger positive value in dichloromethane and a smaller negative value in acetonitrile. The largest contribution to this trend is the significantly more positive $E_{1/2}$ values for the $[Pd(ptas)_2]^{2+/+}$ than $[Pd(mtas)_2]^{2+/+}$ couple in each solvent ($E_{1/2}$ for the two Pd(I/0) couples in each solvent are very similar), indicating that it is the stabilities of the Pd(II) species that have most influence on the differences in $\Delta E_{1/2}$. Again the same observations were made for $[Ni(ptas)_2]^{2+}$ and $[Ni(mtas)_2]^{2+}$ in acetonitrile.[7] The explanation for this trend presumably lies, in part, in the larger steric demands of the ptas ligand. Steric crowding of the bulkier ptas ligands may destabilize the $[M(ptas)_2]^{2+}$ complexes (M = Pd, Ni) relative to the mtas complexes whereas at the larger M(I) centers and for the M(0) complexes with lower coordination number, ligand bulk has little influence on complex stability. Electronic factors may also be important. On the basis of inductive effects, >AsPh is expected to be a weaker σ-donor than the >AsMe group, thus raising the energy of $[M(ptas)_2]^{2+}$ relative to $[M(mtas)_2]^{2+}$. On the other hand, for the lower oxidation state species, the π-acceptor rather than σ-donor properties of ligands are important for determining the stability of the complexes.

Kinetics of the Two One-Electron Steps. The kinetic discrimination of the single electron transfer steps achieved in acetonitrile and, for $[Pd(mtas)_2]^{2+}$, in dichloromethane, relies on the second electrode process being rate-controlling and on unfavorable kinetics for the disproportionation reaction (eq 5). In addition to the expected effects on electrode and homogeneous kinetics of increasing the cyclic voltammetric scan rate and decreasing the solution temperature, kinetic discrimination is facilitated by three other features of the system.

First, the kinetics for the second reduction step are considerably slower in dichloromethane than in acetonitrile. The reasons for this rate retardation are not understood; while ion-pairing was suggested to influence the kinetics of the Ni(II/III) couple in dichloromethane,[7] it seems unlikely that ion-pairing interactions would increase in significance for the lower charged and larger Pd(I) complexes.

Second, the apparent electrode kinetics for $[Pd(ptas)_2]^{+/0}$ are particularly slow. Significantly slower apparent kinetics were also found for the ptas compared to the mtas complex of Ni, and this was attributed to the larger steric bulk of the ptas ligand leading to slower structural rearrangement of the complex. Presumably the same is true for the Pd analogues.

Finally, the sensitivity of the apparent electrode kinetics to the electrode material gives an additional means of tuning the kinetics. As noted earlier, the kinetics generally appear faster at GC, and hence use of a Pt electrode facilitates kinetic discrimination of the two electron-transfer steps. The reason for the marked dependency of the electrode kinetics on electrode material has not been established. However, it might be expected that the arsine ligands will interact most strongly with the Pt electrode, leading to adsorption of products and apparent slowing of electrode kinetics. Alternatively, coordination of $-AsMe_2$ groups to the Pt surface might occur during the electron-transfer steps, slowing down the rate of the requisite structural rearrangements of the complexes.

Conclusions

The monomeric Pd(I) species $[Pd(ptas)_2]^+$ and $[Pd(mtas)_2]^+$ are shown to be thermodynamically stable in dichloromethane over a potential range of *ca.* 180 and 20 mV, respectively.

Stabilization of $[Pd(ptas)_2]^+$ is promoted by the relatively low polarity of the solvent, the steric bulk of the ligand, and the weaker σ-donor power of ptas relative to mtas, which together act to destabilize the Pd(II) complex. In acetonitrile both Pd(I) complexes are unstable with respect to disproportionation. Separate electrode responses can be observed for the Pd(II/I) and Pd(I/0) couples when the kinetics of the Pd(I/0) electrode reaction and the homogeneous disproportionation reaction are slow with respect to the experimental time scale.

Acknowledgment. The authors thank Dr Owen J. Curnow for providing molecular modeling results. Part of this work was undertaken at La Trobe University when A.M.B. was Professor of Chemistry and A.J.D. was on leave from the University of Canterbury. A.J.D. thanks the University of Canterbury for the granting of study leave.

Supporting Information Available: Figures showing (i) the cyclic voltammogram of 0.43 mM $[Pd(ptas)_2]^{2+}$ at a Pt electrode and $\upsilon = 0.05$ V s^{-1}, (ii) cyclic voltammograms of 0.63 mM $[Pd(mtas)_2]^{2+}$ at a GC electrode and scan rates of (a) 0.5, (b) 1, and (c) 50 V s^{-1}, (iii) steady-state voltammograms ($\upsilon = 0.05$ V s^{-1}; $T = 22$ °C) recorded using a GC fiber microelectrode of 0.5 mM $[Pd(mtas)_2]^{2+}$ (a) before and (b) after controlled-potential electrolysis at an applied potential of -1.4 V *vs* Fc^+/Fc. All voltammograms were recorded in acetonitrile−0.1 M Bu_4NPF_6 ($T = 22$ °C) (6 pages). Ordering information is given on any current masthead page.

IC960642G